TITLE: Myofibroblasts in proliferative diabetic retinopathy can originate from infiltrating fibrocytes and through endothelial-to-mesenchymal transition (EndoMT)

AUTHORS: Ahmed M. Abu El-Asrar[a*], MD, PhD; Gert De Hertogh[b], MD, PhD; Kathleen van den Eynde[b] MSc; Kaiser Alam[a], PhD; Katrien Van Raemdonck[c]; Ghislain Opdenakker[c], MD, PhD; Jo Van Damme[c], PhD; Karel Geboes[b], MD, PhD; Sofie Struyf[c], PhD

Affiliations:

[a]Department of Ophthalmology, College of Medicine, King Saud University, Riyadh, Saudi Arabia and *Dr. Nasser Al-Rasheed Research Chair in Ophthalmology.
[b]Laboratory of Histochemistry and Cytochemistry, University of Leuven, KU Leuven, Belgium
[c]Rega Institute for Medical Research, Department of Microbiology and Immunology University of Leuven, KU Leuven, Belgium.

Correspondence to:

Ahmed M. Abu El-Asrar, MD, PhD
Department of Ophthalmology
King Abdulaziz University Hospital
Old Airport Road, P.O. Box 245, Riyadh 11411, Saudi Arabia
Tel: 966-11-4775723 Fax: 966-11-4775724
E-mail: abuasrar@KSU.edu.sa / abuelasrar@yahoo.com

ABSTRACT

Myofibroblasts expressing α-smooth muscle actin (α-SMA) are the key cellular mediator of fibrosis. Fibrovascular epiretinal membranes from patients with proliferative diabetic retinopathy (PDR) are characterized by the accumulation of a large number of myofibroblasts. We explored the hypothesis that proliferating endothelial cells via endothelial-to-mesenchymal transition (EndoMT) and/or bone marrow-derived circulating fibrocytes contribute to the myofibroblast population present in PDR epiretinal membranes. Epiretinal membranes from 14 patients with PDR were studied by immunohistochemistry. All membranes contained neovessels expressing the endothelial cell marker CD31. $CD31^+$ endothelial cells co-expressed the fibroblast/myofibroblast markers fibroblast-specific protein-1 (FSP-1) and α-SMA, indicative for the occurrence of endoMT. In the stroma, cells expressing FSP-1, α-SMA, the leukocyte common antigen CD45, and the myelomonocytic marker CD11b were detected. Double labeling showed co-localization of CD45 with FSP-1 and α-SMA and co-localization of CD11b with α-SMA and matrix metalloproteinase-9, demonstrating the presence of infiltrating fibrocytes. In addition, we investigated the phenotypic changes that take place in human retinal microvascular endothelial cells following exposure to transforming growth factor-β1 (TGF-β1), connective tissue growth factor (CTGF) and the proinflammatory cytokines interleukin-1β (IL-1β) and tumor necrosis factor-α (TNF-α). Retinal microvascular endothelial cells changed morphology upon cytokine exposure, lost the expression of endothelial cell markers (endothelial nitric oxide synthase and vascular endothelial-cadherin) and started to express mesenchymal markers (calponin, snail, transgelin and FSP-1). These results suggest that endothelial cells as well as circulating fibrocytes may differentiate into myofibroblasts in the diabetic eye and contribute to pathologic fibrosis in PDR.

Key words: endothelial-to-mesenchymal transition (EndoMT); fibrocytes; myofibroblasts;

proliferative diabetic retinopathy; endothelial cells; retina

1. Introduction

Ischemia-induced pathologic growth of new blood vessels and expansion of extracellular matrix (ECM) in association with the outgrowth of fibrovascular epiretinal membranes at the vitreoretinal interface is the pathological hallmark in proliferative diabetic retinopathy (PDR), and often leads to catastrophic loss of vision due to vitreous hemorrhage and/or traction retinal detachment. Although the etiology of fibrotic disorders is quite diverse, and their pathogenesis is variable and dependent on the causative agent or initiating event, a common feature is the presence of large numbers of myofibroblasts and abnormal accumulation of ECM in the affected tissue(s). Myofibroblasts, the key cellular mediators of fibrosis, are contractile cells, characterized by the expression of α-smooth muscle actin (α-SMA), and their presence is a marker of progressive fibrosis. They have the capacity to produce several ECM components including collagen resulting in fibrosis (Wynn, 2008). Such myofibroblasts, sometimes termed "activated fibroblasts", are known to be present in the stromal compartment of most invasive human cancers, in areas of chronic inflammation, and in tissues undergoing the remodeling seen during wound healing (Wynn, 2008). In the epiretinal membranes from patients with PDR, inflammatory and fibrotic changes are characterized by the presence of inflammatory cells and α-SMA-expressing myofibroblasts in the stromal compartment (Abu El-Asrar et al., 2006, 2007, 2013).

The origin(s) of myofibroblasts responsible for the exaggerated and uncontrolled production of ECM proteins in PDR epiretinal membranes has not been completely elucidated. Investigations of other fibrotic diseases suggest that the activated fibroblasts or myofibroblasts can probably derive from diverse origins, depending on the organ and on the pathology. Increasing evidence suggests that endothelial cells may undergo endothelial-to-mesenchymal transition (EndoMT) or endothelial-to-myofibroblast transition under physiological, as well as pathological circumstances (Piera-Velasquez et al., 2011; He et al., 2013). During EndoMT, endothelial cells lose their adhesion and apical-basal polarity to form highly invasive migratory, spindle-shaped elongated mesenchymal cells. More importantly, biochemical changes accompany these distinct changes in cell polarity and morphology, including the decreased expression of endothelial markers, such as CD31, vascular endothelial (VE)-cadherin, and endothelial nitric oxide synthase (eNOS) and the acquisition of mesenchymal markers, such as α-SMA, fibroblast-specific protein-1 (FSP-1, also known as S100A4), calponin, and smooth muscle protein 22 α (SM22α) or transgelin (Piera-

Velasquez et al., 2011; He et al., 2013). The cells undergoing transition may contain both endothelial and mesenchymal properties. For instance, Zeisberg et al. (2008) postulated that co-labeling of tissue with the endothelial marker CD31 and the mesenchymal markers α-SMA and FSP-1 reliably identifies myofibroblasts derived via EndoMT. It was demonstrated that transforming growth factor (TGF)-β1 treatment of mouse pancreatic microvascular endothelial cells and mouse lung endothelial cells induced EndoMT (Li et al., 2009; Zeisberg et al., 2007) and that snail, a zinc finger-containing transcription factor, mediates the actions of endogenous TGF-β1 signals that induce EndoMT (Piera-Velasquez et al., 2011; He et al., 2013). In addition, the inflammatory cytokines interleukin-1β (IL-1β) or tumor necrosis factor-α (TNF-α) induced permanent transformation of human epithelioid dermal microvascular endothelial cells into myofibroblasts (Chaudhuri et al., 2007). Furthermore, co-stimulation with IL-1β and TGF-β2 caused synergistic induction of EndoMT in human umbilical vein endothelial cells (Maleszewska et al., 2013). Recently, several studies provided strong evidence for the prominent participation of EndoMT in the generation of activated myofibroblasts in animal models of renal, cardiac, pulmonary, hepatic and intestinal fibrosis (Piera-Velasquez et al., 2011; He et al., 2013). Furthermore, EndoMT emerges as a possible source of cancer-associated fibroblasts (Zeisberg et al., 2007). In diabetic eyes, however, EndoMT has not yet been investigated.

In addition to EndoMT, several studies demonstrated that circulating bone marrow-derived fibrocytes traffic to sites of tissue injury, differentiate into myofibroblasts, and contribute to collagen deposition and fibrosis (Keeley et al., 2011). Circulating fibrocytes express the hematopoietic stem cell marker CD34, the common leukocyte marker CD45 and the myeloid marker CD11b in conjunction with the fibroblast markers vimentin, collagen I, collagen III and fibronectin (Keeley et al., 2011). The expression of α-SMA is a marker of differentiation of fibrocytes into myofibroblasts (Keeley et al., 2011).

In the present study, we explored the hypothesis that both EndoMT and bone marrow-derived circulating fibrocytes contribute to the myofibroblast population present in the epiretinal membranes from patients with PDR. To identify fibrocytes that have undergone local differentiation into myofibroblasts, we performed double-labeling experiments to reveal cells co-expressing CD45/α-SMA, CD45/FSP-1, and CD11b/α-SMA. In addition, we performed CD31/FSP-1 and CD31/α-SMA double-labeling to gain insights into possible EndoMT. Finally, we demonstrated that phenotypic changes take place in human retinal

microvascular endothelial cells (HRMEC) following exposure to TGF-β1, and the proinflammatory cytokines IL-1β and TNF-α. In the stimulated cell cultures, retinal endothelial cells changed morphology, down-regulated endothelial cell markers and upregulated mesenchymal/myofibroblast markers. These findings corroborate the hypothesis that EndoMT can contribute to the fibrotic process occurring during PDR.

2. Materials and Methods

2.1. Epiretinal membrane specimens

Epiretinal fibrovascular membranes were obtained from 14 patients with PDR during pars plana vitrectomy for the repair of tractional retinal detachment. The severity of retinal neovascular activity was graded clinically at the time of vitrectomy using previously published criteria (Aiello et al., 1994). Neovascularization was considered active if there were visible perfused new vessels on the retina or optic disc and present within tractional epiretinal membranes. Neovascularization was considered inactive (involuted) if only nonvascularized white fibrotic epiretinal membranes were present. Active PDR was present in 5 patients and inactive PDR was present in 9 patients. Membranes were fixed in 10% formalin solution and embedded in paraffin.

The study was conducted according to the tenets of the Declaration of Helsinki. All patients were candidates for vitrectomy as a surgical procedure and signed a preoperative informed written consent approving the use of the excised epiretinal membranes for further analysis and clinical research. The study design and the protocol were approved by the Research Centre and Institutional Review Board of the College of Medicine, King Saud University.

The sections from the control patients were obtained from patients treated at the University Hospital, University of Leuven, Belgium, in full compliance with tenets of the Declaration of Helsinki. We used archived material and patients gave written consent at admission for the use of the leftover material in studies. The Ethics Committee of the University Hospital, University of Leuven approved this consent procedure.

2.2. Immunohistochemical staining

For CD31 and α-SMA detection, antigen retrieval was performed by boiling the sections in citrate based buffer (BOND Epitope Retrieval Solution 1, pH 5.9 – 6.1; Leica) for 20 minutes. For FSP-1, CD45, CD11b and matrix metalloproteinase-9 (MMP-9) detection, antigen retrieval was performed by boiling the sections in Tris/EDTA buffer (BOND Epitope Retrieval Solution 2, pH 9; Leica) for 20 minutes. Subsequently, the sections were incubated with the monoclonal and polyclonal antibodies listed in Table 1. Optimal working concentrations and incubation times for the antibodies were determined earlier in pilot experiments. The sections were then incubated for 20 minutes with a post primary IgG linker followed by an alkaline phosphatase-conjugated polymer. The reaction product was visualized by incubation for 15 minutes with the Fast Red chromogen (BOND Polymer Refine Red Detection Kit; Leica), resulting in bright-red immunoreactive sites. The slides were then faintly counterstained with Mayer's hematoxylin.

To identify the phenotype of cells expressing FSP-1, α-SMA and MMP-9, sequential double immunohistochemistry was performed. The stronger antigen retrieval (Tris/EDTA buffer) of the two single stainings was used when combining them in double staining. Therefore, only one antigen retrieval was performed per each double staining. The sections were incubated with the first primary antibody (anti-CD31, anti-CD45 and anti-CD11b) and subsequently treated with peroxidase conjugated secondary antibody. Immunoreactive sites were visualized with 3,3'-diaminobenzidine tetrahydrochloride. Incubation of the second primary antibody (anti-FSP-1, anti-α-SMA and anti-MMP-9) was followed by treatment with alkaline phosphatase conjugated secondary antibody. Finally, the sections were treated with Fast Red colour solution. No counterstain was applied.

Omission or substitution of the primary antibody with an irrelevant antibody from the same species and staining with chromogen alone were used as negative controls. Sections from patients with glioblastoma were used as positive controls to optimize the immunohistochemical staining methods.

2.3. Quantitation

Immunoreactive blood vessels and cells were counted in five representative fields, using an eyepiece calibrated grid in combination with the 40x objective. These representative

fields were selected based on the presence of immunoreactive blood vessels and cells. With this magnification and calibration, immunoreactive blood vessels and cells present in an area of 0.33 x 0.22 mm² were counted.

2.4. Differentiation of retinal microvascular endothelial cells

HRMEC were purchased from Cell Systems (Kirkland, WA) and cultured as described previously (Nawaz et al., 2013) in endothelial basal medium-2 (EBM-2) enriched with endothelial growth medium-2 MV Bulletkit, containing, besides fetal calf serum [FCS; final concentration 5% (v/v)], the growth factors epidermal growth factor, vascular endothelial growth factor (VEGF), basic fibroblast growth factor and insulin-like growth factor 1 (Lonza, Verviers, Belgium). Three days after seeding in 6-well plates, differentiation of HRMEC was induced by addition of human recombinant IL-1β, human recombinant TNF-α, human recombinant TGF-β1 or human recombinant connective tissue growth factor (CTGF) (all from PeproTech, Rocky Hill, NJ) or combinations thereof and replacement of the growth-factor enriched endothelial cell growth medium by EBM-2 supplemented with 3% FCS. As a control to preserve the endothelial cell type, cultures in one well of each plate were contained in the endothelial cell growth medium supplemented with 10 ng/ml of VEGF. The differentiation medium was replaced every two days. After 4 days of stimulation, cell morphology and gene expression were investigated. Changes in cell morphology were documented using an Axiovert 200M inverted microscope, equipped with an EC Plan-Neofluar 10× phase contrast objective (Carl Zeiss, Jena, Germany).

2.5. Quantitative measurement of gene expression

Changes in gene expression 4 days after exposure of HRMEC to cytokines were studied using quantitative real-time PCR. Total RNA was extracted with the RNeasy kit (Qiagen, Hilden, Germany) according to the procedures of the manufacturer and quantified by UV absorption. RNA was converted into cDNA by reverse transcription using the high capacity cDNA Reverse Transcription kit from Applied Biosystems (Life Technologies, Gent, Belgium). Quantitative RT-PCR analysis was performed with the TaqMan gene expression master mix from Applied Biosystems and primers and probes, supplied as PrimeTime qPCR assays, by Integrated DNA Technologies (Table 2) on 50 ng of cDNA in an Applied Biosystems 7500 fast real-time PCR system. The relative abundance of transcripts was determined by the $2^{-\Delta\Delta Ct}$ method. ΔCt values were calculated using 18S ribosomal RNA

as a reference (assay no. Hs.PT.45.122532.g). Upregulation or down-regulation of a gene of interest was calculated relative to the control culture in which the full endothelial growth medium was replaced by EBM-2 + 3% FCS without addition of cytokine(s). At least four independent experiments were performed in which each condition was tested in duplicate.

2.6. Western blot analysis

HRMEC were maintained in complete serum free media (Cat. No. SF-4Z0-500, Cell Systems) supplemented with Rocket fuel (Cat No. SF-4ZO-500, Cell systems), culture boost (Cat. No. 4CB-500, Cell Systems) and antibiotics (Cat. No. 4ZO-643, Cell Systems) at 37°C in a humidified atmosphere with 5% CO_2. When HRMEC cells reached 80% confluency, cultures were starved overnight in a minimal medium containing antibiotics, 0.5% rocket fuel and without culture boost. Following starvation, HRMEC cells were left untreated or treated in minimal starvation medium either with TNF-α, IL-1β, TGF-β1, CTGF (ab50044, Abcam, Cambridge, CB4 0FL,UK) or with a cocktail of cytokines containing either TNF-α plus IL-1β plus TGF-β1 or TNF-α plus IL-1β plus CTGF. All conditions were tested in triplicate. After every 48 hours, the media of all the groups with respective cytokines were replaced. Cells were harvested after 6 days for analysing the expression pattern of various proteins involved in EndoMT. HRMEC cells were lysed with RIPA buffer [50 mM Tris/HCl, pH 7.5, 150 mM NaCl, 1% (v/v) nonidet P40 (NP40), 0.5% sodium deoxycholate, 0.1% SDS and protease inhibitor "Complete without EDTA" (Roche, Mannheim, Germany)]. Whole cell extracts were centrifuged at 12,000 ×g for 10 minutes at 4°C. The supernatants were collected and protein concentrations were measured using the DC protein assay kit (Bio-Rad Laboratories, Hercules, CA). Whole cell extracts containing 50 μg of protein were separated on 8–12% SDS-polyacrylamide gels and were transferred onto nitrocellulose membranes. Blocking was performed with 5% skim milk in Tris buffered saline (TBS-T) (50 mM Tris-Cl, pH 7.6, 150 mM NaCl, 0.05% Tween 20) for 1 hour. For the detection of eNOS, VE-cadherin and FSP-1, the membranes were incubated overnight at 4°C with the respective primary antibody. The antibodies used were goat polyclonal anti-eNOS (1:1000, Cat. no. AF950, R&D Systems, Minneapolis, MN), mouse monoclonal anti-VE-cadherin (1 : 500, Cat no. SC-9989, Santa Cruz Biotechnology, Inc., Santa Cruz, CA), and rabbit polyclonal anti-FSP-1 (1:500, Cat no. SC-292281, Santa Cruz Biotechnology, Inc.,). After overnight incubation with primary antibodies, the membranes were washed four times with TBS-T (5 minutes each). Then the membranes were incubated with respective secondary antibodies at room temperature for

1 hour. Anti-goat horseradish peroxidase (HRP)-conjugated antibody (1 : 3000, SC-2768), anti-mouse HRP-conjugated antibody (1 : 3000, SC-2005), and anti-rabbit HRP-conjugated antibody (1 : 3000, SC-2004) were purchased from Santa Cruz Biotechnology, Inc.. After incubations with secondary antibodies, membranes were washed four times with TBS-T (5 minutes each) and the intensity of bands was visualized on a high-performance chemiluminescence machine (G: Box Chemi-XX8 from Syngene, Synoptic Ltd. Cambridge, UK) by using enhanced chemiluminescence plus Luminol (SC-2048, Santa Cruz). The membranes that were used to probe e-NOS, VE-cadherin and FSP-1 were re-probed for β-actin (mouse monoclonal anti-β-actin antibody (C4), 1:2000 SC-47778, Santa Cruz) to verify equal loading. Band intensities were quantified using image software GeneTools (Syngene by Synoptic Ltd. Cambridge, UK) and ratios for marker expression over β-actin expression were calculated. Statistical analysis was done on the results obtained from three independent experiments and each experiment was in triplicate.

2.7. Statistical Analysis

Data are presented as the mean ± standard deviation (SD), unless otherwise indicated (Fig. 6). The non-parametric Mann-Whitney U test was used to compare means from two independent groups. Pearson correlation coefficients were computed to investigate correlations between variables. A p-value less than 0.05 indicated statistical significance. SPSS version 19.0 (IBM Inc., Chicago, IL) and program 3S from the BMDP 2007 Statistical Package were used for the statistical analyses.

3. Results

3.1. Neovascularization and expression of mesenchymal markers in epiretinal membranes from patients with PDR

The level of vascularization in epiretinal membranes was determined by immunodetection of the endothelial cell marker CD31. No staining was observed in the negative control slides, in which an irrelevant primary antibody was used (Fig. 1A). However, using anti-CD31, all membranes showed blood vessels positive for this endothelial cell marker (Fig. 1B), with a mean number of 43±45 (range, 12-125). Fibrotic tissue is often

infiltrated by mesenchymal cells (expressing α-SMA and FSP-1) secreting new ECM. Strong immunoreactivity for FSP-1 was present in all membranes and was observed in the cytoplasm of stromal cells (Fig. 1C) and vascular endothelial cells (Fig. 1D, E). The number of FSP-1 immunoreactive stromal cells ranged from 10 to 195, with a mean number of 75±64. The number of FSP-1 immunoreactive blood vessels ranged from 1 to 30, with a mean number of 10±10. Similarly, cytoplasmic immunoreactivity for α-SMA was noted in stromal cells and vascular endothelial cells (Fig. 1F, G).

The mean number of blood vessels expressing CD31, was significantly higher in membranes from patients with active PDR (98±26) than in membranes from patients with inactive PDR (13±8) (p=0.001). In addition, the mean number of stromal cells expressing FSP-1 was significantly higher in membranes from patients with active PDR (139±43) than in membranes from patients with inactive PDR (39±41) (p=0.004). However, the difference between the mean numbers of blood vessels expressing FSP-1 in membranes from patients with active PDR (14±7) and in membranes from patients with inactive PDR (8±10) was not significant (p=0.112). A significant positive correlation was detected between the numbers of blood vessels expressing CD31 and the numbers of stromal cells expressing FSP-1 (r=0.77, p=0.001). On the other hand, the correlation between the numbers of blood vessels expressing CD31 and the numbers of blood vessels expressing FSP-1 was not significant (r=0.47, p=0.093).

3.2. $CD45^+/FSP\text{-}1^+$ and $CD45^+/\alpha\text{-}SMA^+$ double-positive cells in epiretinal membranes from patients with PDR

To verify whether bone marrow-derived circulating fibrocytes contribute to the myofibroblast population present in the epiretinal membranes from patients with PDR, we performed immunohistochemistry with anti-CD45, anti-FSP-1 and anti-α-SMA antibodies. All membranes showed stromal cells expressing the leukocyte common antigen CD45, in their plasma membrane (Fig. 2A). The number of CD45 immunoreactive stromal cells ranged from 5 to 230, with a mean number of 85±99. The mean numbers of stromal cells expressing CD45, were significantly higher in membranes from patients with active PDR (177±113) than in membranes from patients with inactive PDR (34±38) (p=0.004). A significant positive correlation was detected between the number of blood vessels expressing CD31 and the number of stromal cells expressing CD45 (r=0.81, p=0.001). To identify fibrocytes that had

undergone local differentiation into mesenchymal cells, double-labeling experiments were performed. $CD45^+$ cells (brown) co-expressing FSP-1 (red) (Fig. 2B) and α-SMA (red) (Fig. 2C, D) were detected.

3.3. $CD11b^+/\alpha$-SMA^+ and $CD11b^{+/}MMP$-9^+ double-positive cells in epiretinal membranes from patients with PDR

Next we investigated whether fibrocytes are recruited into the stroma of diabetic epiretinal membranes and *in situ* differentiate into myofibroblasts. Immunoreactivity for the myeloid marker CD11b, present on fibrocytes, was identified in all membranes and was noted in stromal cells (Fig. 3A) and vascular endothelial cells (Fig. 3B). The number of immunoreactive stromal cells ranged from 10 to 160, with a mean number of 58±43. The number of immunoreactive blood vessels ranged from 4 to 65, with a mean number of 23±17. The mean number of stromal cells expressing CD11b, was significantly higher in membranes from patients with active PDR (87±43) than in membranes from patients with inactive PDR (42±35) ($p=0.029$). Similarly, the mean number of blood vessels expressing CD11b, was significantly higher in membranes from patients with active PDR (37±16) than in membranes from patients with inactive PDR (12±12) ($p=0.012$). A significant positive correlation was detected between the numbers of blood vessels expressing CD31 and either the numbers of stromal cells expressing CD11b ($r=0.55$, $p=0.048$) or blood vessels expressing CD11b ($r=0.67$, $p=0.009$). Double immunohistochemistry indicated that CD11b-positive cells (brown) co-expressed α-SMA (red) (Fig. 3C, D) and MMP-9 (red) (Fig. 3E).

3.4. $CD31^+/FSP\text{-}1^+$ and $CD31^+/\alpha$-SMA^+ double-positive cells in epiretinal membranes from patients with PDR

Double immunohistochemistry revealed that some endothelial cells expressing the endothelial cell marker CD31 (brown) co-expressed FSP-1 (red) (Fig. 4A, B) and α-SMA (red) (Fig. 4C, D). These findings suggest that endothelial cells are undergoing phenotypic conversion and are beginning to acquire fibroblast/myofibroblast markers.

3.5. Cultured retinal microvascular endothelial cells can acquire characteristics of myofibroblasts upon appropriate cytokine treatment

To verify the hypothesis that EndoMT indeed occurs in epiretinal membranes of diabetic patients, we tested whether cultured HRMEC could also be reprogrammed. We stimulated HRMEC with 10 ng/ml TGF-β1, 30 ng/ml TNF-α, 10 ng/ml IL-1β or 0.5 μg/ml CTGF alone or combinations thereof and concurrently removed the endothelial growth factors from the culture medium (see Materials and Methods). We compared cell cultures maintained for 4 days in those conditions to cultures kept in the presence of full endothelial growth medium supplemented with 10 ng/ml of VEGF. Figure 5 shows that the deprived cells changed their morphology drastically in the presence of TNF-α plus IL-1β, regardless of the presence or absence of TGF-β1. Reduced cell-to-cell contacts were observed and the cells resembled myofibroblasts with an irregular, elongated shape. On the other hand, CTGF did not change the morphology of the cells (data not shown). We isolated RNA from the cell cultures and analysed the modulation of gene expression in response to the altered culture conditions (Fig. 6). We first studied the mRNA expression levels of the endothelial cell markers CD31, VE-cadherin and eNOS. Treatment with TNF-α plus IL-1β or TNF-α plus IL-1β plus TGF-β1 resulted in a significant downregulation of VE-cadherin and eNOS gene expression, whereas no change in CD31 expression was detected. Concurrently, the myofibroblast-like cells upregulated transcription of the mesenchymal genes snail, transgelin and calponin in response to combined stimulation (n=4, Fig. 6), or in response to IL-1β alone (n=2, data not shown). The fact that CD31 expression levels remained unchanged suggests that the transition to myofibroblasts is not fully complete yet and that we obtained an intermediate differentiation status, similar to the phenotype of cells detected by immunohistochemistry ($CD31^+$/α-SMA^+ and $CD31^+$/$FSP\text{-}1^+$) in the pathologic membranes.

The observed changes in mRNA levels in the cultured HRMEC were confirmed by Western blot analysis (Fig. 7). On day 6, Western blot analysis revealed significant dowregulation of eNOS protein in response to TNF-α, IL-1β, TGF-β1 or TNF-α plus IL-1β plus TGF-β1 treatment. Similarly, IL-1β, TGF-β1 or TNF-α plus IL-1β plus TGF-β1 treatment resulted in a significant downregulation of VE-cadherin. Treatment with TNF-α, IL-1β, TGF-β1 or TNF-α plus IL-1β plus TGF-β1 resulted in a significant upregulation of FSP-1 protein levels. Treatment of HRMEC with CTGF alone did not affect the expression of

eNOS, VE-cadherin and FSP-1 as compared to untreated control (data not shown). In conclusion, our data support the occurrence of EndoMT in cultures of HRMEC.

4. Discussion

Here, we demonstrated for the first time that endothelial cells in epiretinal fibrovascular membranes from patients with PDR contribute to the emergence of fibroblasts/myofibroblasts via the process of EndoMT. We report that some endothelial cells expressing CD31 co-express the fibroblast marker FSP-1 and the myofibroblast marker α-SMA. The presence of $CD31^{+/}FSP\text{-}1^{+}$ and $CD31^{+}/\alpha\text{-}SMA^{+}$ cells indicates an intermediate stage of EndoMT (Zeisberg et al., 2007, 2008). Our observations suggest that EndoMT plays a role in creating fibroblasts and myofibroblasts responsible for fibrosis and progression of PDR. These findings also suggest that EndoMT contributes to the loss of endothelial cells in PDR epiretinal membranes and the spontaneous regression of new blood vessels in patients with end-stage PDR. These findings raise the possibility that inhibiting EndoMT may be an effective therapy for delaying the progression of fibrosis associated with PDR.

Our *in vivo* findings are consistent with previous *in vitro* data demonstrating that high glucose treatment induced EndoMT in human aortic endothelial cells and human umbilical vein endothelial cells (Tang et al., 2010, 2013; Widyantoro et al., 2010). High glucose treatment reduced VE-cadherin levels and induced the expression of FSP-1 protein, and co-localization of both CD31 and FSP-1 (Tang et al., 2010, 2013; Widyantoro et al., 2010). EndoMT was also induced in a mouse pancreatic microvascular endothelial cell line in the presence of advanced glycation end products(Li et al., 2010). In our *in vitro* experiments we were also able to demonstrate differentiation of retinal microvascular endothelial cells into spindle-shaped cells displaying downregulation of the endothelial cell markers, such as eNOS and VE-cadherin and upregulation of the mesenchymal markers calponin, snail, transgelin and FSP-1. In Fig. 6 CD31 expression was not yet downregulated on day 4, but several authors report co-expression of CD31 with mesenchymal markers, before CD31 expression is downregulated at a later stage of EndoMT (Zeisberg et al., 2007; Tang et al., 2010). Besides, also in the immunohistochemical analysis of the diabetic epiretinal membranes (Fig. 4) co-expression of CD31 with α-SMA and FSP-1 was detected. In view of the above mentioned literature, we also tested exposure of the endothelial cells to high glucose levels. However,

we did not observe a clear effect on the cell cultures, neither at a morphological level, nor in gene expression (data not shown). This discrepancy might be explained by the fact that HRMEC used in our study respond differently compared to other types of endothelial cells.

In addition, on the basis of animal experiments it has previously been suggested that EndoMT plays an important role in the progression of diabetes-induced renal fibrosis (Zeisberg et al., 2008; Li et al., 2009) and cardiac fibrosis (Tang et al., 2013; Widyantoro et al., 2010). In a mouse model of streptozotocin (STZ)-induced diabetic nephropathy, Zeisberg et al. (2008) demonstrated that a considerable proportion of all FSP-1$^+$ fibroblasts and α-SMA$^+$ myofibroblasts co-expressed the endothelial marker CD31. Li et al. 2009) confirmed that EndoMT occurs and contributes to the generation of myofibroblasts in early STZ-induced diabetic nephropathy in mice. These findings strongly indicate the existence of endothelial-origin fibroblasts/myofibroblasts in diabetic nephropathy and suggest that EndoMT may be a pathway leading to interstitial fibrosis in diabetic nephropathy. Similarly, recent studies demonstrated that STZ-induced cardiac fibrosis is associated with the emergence of fibroblasts from endothelial cells. Labeling experiments showed that CD31-labeled endothelial cells co-expressed FSP-1 (Tang et al., 2013; Widyantoro et al., 2010).

In the present study, we described the *in situ* localization of FSP-1 in leukocytes, expressing the leukocyte common antigen CD45, as well as in endothelial cells in epiretinal membranes from patients with PDR. In accordance with our results, previous studies reported that FSP-1$^+$cells are also increased in experimental models of renal fibrosis (He et al., 2013; Zeisberg et al., 2008), cardiac fibrosis (Tang et al., 2013; Widyantoro et al., 2010), liver diseases (Österreicher et al., 2011), cancer (Zeisberg et al., 2007) and vein grafts (Cheng et al., 2012). In a rat model of renal peritubular inflammation, FSP-1$^+$ cells consistently co-expressed CD45. In addition, FSP-1 stained endothelial cells in the mouse model of renal peritubular inflammation (Le et al., 2005). In liver diseases, FSP-1$^+$ cells co-expressed markers of the myeloid-monocytic lineage (macrophages and/or dendritic cells) (Österreicher et al., 2011). In vein grafts, FSP-1$^+$ cells also stained positively for CD45 and CD11b (Österreicher et al., 2011). These findings indicate that FSP-1$^+$ stromal cells in PDR epiretinal membranes are of hematopoietic origin.

In fibrovascular epiretinal membranes from patients with PDR, we demonstrated accumulation of mononuclear cells of monocyte/macrophage lineage expressing CD45 and

CD11b. A subset of these cells co-expressed FSP-1 and α-SMA, thus exhibiting mesenchymal cell characteristics attributed to fibrocytes (Keeley et al., 2011). We concluded that circulating mesenchymal precursors of a monocyte/macrophage lineage, including fibrocytes, are another source of myofibroblasts and thus contribute to fibrosis in PDR. TGF-β1 plays an important role during the transdifferentiation of monocytes/macrophages expressing CD11b into cells expressing the myofibroblast markers α-SMA and calponin (Ninomiya et al., 2006). The chemokine receptor-ligand pair CXCR4-stromal cell-derived factor-1 (SDF-1/CXCL12) has been shown to play a particularly important role in the homing of circulating fibrocytes to sites of fibrosis (Keeley et al., 2011). In previous studies, we demonstrated expression of the CXCL12/CXCR4 chemokine axis in PDR epiretinal membranes (Abu El-Asrar et al., 2010, 2011).

New blood vessels in PDR epiretinal membranes are derived from sprouting from preexisting endothelial cells (angiogenesis) and circulating bone marrow-derived endothelial precursor cells (vasculogenesis) (Ninomiya et al., 2006; Abu El-Asrar et al., 2010, 2011). In the present study, we demonstrated that vascular endothelial cells in PDR epiretinal membranes expressed the myelomonocytic marker CD11b. These findings suggest that bone marrow-derived $CD11b^+$ myelomonocytic cells play an important role in PDR vasculogenesis. In addition, $CD11b^+$ cells co-expressed MMP-9. This observation corroborates several recent studies reporting that $CD11b^+$ cells have multiple tumor-promoting effects. They show high proangiogenic activity as they actively secrete MMP-9, which facilitates endothelial cell migration and liberates matrix-bound growth factors, such as VEGF. In addition, $CD11b^+$ cells directly differentiate and incorporate in the vascular endothelium, promoting tumor vascularization and tumor progression (Yang et al., 2004; Laurent et al., 2011; Ahn and Brown, 2008). Furthermore, several studies demonstrated an essential role for MMP-9 in mediating myofibroblast invasion (Turner et al., 2007) and that fibrocytes expressed high levels of MMP-9 and their migration was MMP-dependent (Sato et al., 2009). In addition, circulating monocytic cells were recently shown to interact with endothelial cells of pulmonary capillaries in a mouse model of acute lung capillary injury and repair. Circulating monocytic cells were shown to express VEGF, to move into close apposition to adjacent capillary endothelium and to fuse to endothelial plasmalemmal membranes and to the endothelial cells of regenerating capillaries after injury. The expression of CXCR4 by the circulating monocytic cells, and of CXCL12 by adjacent endothelial cells, demonstrates a mechanism for retention of these cells at the capillary surface. Myeloid VEGF

receptor-2^+ $CD11b^+$ precursors are identified within the circulating monocytic cell population (Jones and Capen, 2012, 2014). In previous studies we demonstrated the presence of endothelial cells expressing CXCL12 and stromal cells expressing CXCR4 and VEGF receptor-2 in fibrovascular epiretinal membranes from patients with PDR (Abu El-Asrar et al., 2010, 2011).

As both pro-inflammatory and pro-fibrotic mechanisms contribute to the progression of PDR (Abu El-Asrar, et al., 2006, 2007, 2013), we hypothesized that they also interact in the regulation of EndoMT. Therefore, we investigated the pro-EndoMT effect of TGF-β1 in the context of inflammatory TNF-α and IL-1β co-stimulation. Indeed, co-stimulation with the pro-inflammatory cytokines TNF-α and IL-1β and the pro-fibrotic cytokine TGF-β1 caused synergistic induction of the mesenchymal marker transgelin, and possibly calponin, in HRMEC. However, no additive/synergistic effect of TGF-β1 on the combination of TNF-α plus IL-1β was observed in downregulating the endothelial markers eNOS and VE-cadherin (Fig. 6). Our findings suggest that the ocular microenvironment in PDR at the verge between inflammation and tissue remodeling can strongly promote the process of EndoMT.

In conclusion, these findings suggest that EndoMT and circulating bone marrow-derived fibrocytes contribute to the accumulation of myofibroblasts and the development and progression of fibrosis in PDR. A greater understanding of the molecular mechanisms involved in the EndoMT process and modulating the activity of fibrocytes and the subsequent pharmacological blockade of these pathways may represent a novel therapeutic approach to retard the progression of fibrosis associated with PDR.

Conflicts of Interest: None

Authorship contribution

- Abu El-Asrar AM: Conceived and designed the research study, analysed the data, wrote the manuscript, critically reviewed and revised the manuscript and raised funding.
- De Hertogh G: Designed the research study, analysed the data, critically reviewed and revised the manuscript.
- Van den Eynde: Performed the experiments, critically reviewed and revised the manuscript.
- Alam K: Performed the experiments, critically reviewed and revised the manuscript.
- Van Raemdonck K: Performed the experiments, critically reviewed and revised the manuscript.
- Opdenakker G: Analysed the data, critically reviewed and revised the manuscript.
- Van Damme J: Analysed the data, critically reviewed and revised the manuscript and raised the funding.
- Geboes K: Analysed the data, critically reviewed and revised the manuscript.
- Struyf S: Conceived and designed the research study, analysed the data, critically reviewed and revised the manuscript and raised funding.

Acknowledgements

The authors would like to thank Isabelle Ronsse for excellent technical assistance and Ms. Connie Unisa-Marfil for secretarial work. This work was supported by Dr. Nasser Al-Rasheed Research Chair in Ophthalmology (Abu El-Asrar AM), as well as by the Fund for Scientific Research of Flanders (FWO-Vlaanderen project G.0764.14 and G.0773.13), the Interuniversity Attraction Poles Programme initiated by the Belgian Science Policy Office (I.A.P. project P7/40) and the Concerted Research Actions of the Regional Government of Flanders (GOA13/014).

References

Abu El-Asrar, A.M., Missotten, L., Geboes, K., 2007. Expression of hypoxia-inducible factor-1 alpha and the protein products of its target genes in diabetic fibrovascular epiretinal membranes. Br. J. Ophthalmol. 91, 822-826.

Abu El-Asrar, A.M., Mohammad, G., De Hertogh, G., Nawaz, M.I., Van den Eynde, K., Siddiquei, M.M., Strufy, S., Opdenakker, G., Geboes, K., 2013. Neurotrophins and neurotrophin receptors in proliferative diabetic retinopathy. PLoS One 8, e65472.

Abu El-Asrar, A.M., Struyf, S., Kangave, D., Van Damme, J., 2006. Chemokines in proliferative diabetic retinopathy and proliferative vitreoretinopathy. Eur. Cytokine Netw. 17, 155-165.

Abu El-Asrar, A.M., Struyf, S., Opdenakker, G., Van Damme, J., Geboes, K., 2010. Expression of stem cell factor/c-kit signaling pathway components in diabetic fibrovascular epiretinal membranes. Mol. Vis. 16, 1098-1107.

Abu El-Asrar, A.M., Struyf, S., Verbeke, H., Van Damme, J., Geboes, K., 2011. Circulating bone-marrow-derived endothelial precursor cells contribute to neovascularization in diabetic epiretinal membranes. Acta Ophthalmol. 89, 222-228.

Ahn, G.O., and Brown, J.M., 2008. Matrix metalloproteinase-9 is required for tumor vasculogenesis but not for angiogenesis: Role of bone marrow-derived myelomonocytic cells. Cancer Cell 13, 193-205.

Aiello, L.P., Avery, R.L., Arrigg, P.G., Keyt, B.A., Jampel, H.D., Shah, S.T., Pasquale, L.R., Thieme, H., Iwamoto, M.A., Park, J.E., Nguyen, H.V., Aiello, L.M., Ferrara, N., King, G.L., 1994. Vascular endothelial growth factor in ocular fluid in patients with diabetic retinopathy and other retinal disorders. N. Engl. J. Med. 331, 1480-1487.

Chaudhuri, V., Zhou, L., Karasek, M., 2007. Inflammatory cytokines induce the transformation of human dermal microvascular endothelial cells into myofibroblasts: a potential role in skin fibrogenesis. J. Cutan. Pathol. 34, 146-153.

Cheng, J., Wang, Y., Liang, A., Jia, L., Du, J., 2012. FSP-1 silencing in bone marrow cells suppresses neointima formation in vein graft. Circ. Res. 110, 230-240.

He, J., Xu, Y., Koya, D., Kanasaki, K., 2013. Role of the endothelial-to-mesenchymal transition in renal fibrosis of chronic kidney disease. Clin. Exp. Nephrol. 17, 488-497.

Jones R.C., and Capen D.E., 2012 A quantitative ultrastructural study of circulating (monocytic) cells interacting with endothelial cells in high oxygen-injured and spontaneously re-forming (FVB) mouse lung capillaries. Ultrastruct. Pathol. 36, 260-279.

Jones R., and Capen D.E., 2014. Imaging circulating monocytic cells fusing to endothelial cells in acutely injured and regenerating capillaries. Ultrastruct. Pathol. 38, 93-103.

Keeley, E., Mehrad, B., Strieter, R.M., 2011. The role of fibrocytes in fibrotic diseases of the lungs and heart. Fibrogenesis Tissue Repair 4, 2.

Laurent, J., Faes-van't Hull, E., Touvrey, C., Kuonen, F., Lan, Q., Lorusso, G., Doucey, M.A., Ciarloni, L., Imaizumi, N., Alghisi, G.C., Fagiani, E., Zaman, K., Stupp, R., Shibuya, M., Delaloye, J.F., Christofori, G., Ruegg, C., 2011. Proangiogenic factor PIGF programs CD11b+ myelomonocytes in breast cancer during differentiation of their hematopoietic progenitors. Cancer Res. 71, 3781-3791.

Le Hir, M., Hegyi, I., Cueni-Loffing, D., Loffing, J., Kaissling, B., 2005. Characterization of renal interstitial fibroblast-specific protein 1/S100A4-positive cells in healthy and inflamed rodent kidneys. Histochem. Cell Biol. 123, 335-346.

Li, J., Qu, X., Bertram, J.F., 2009. Endothelial-myofibroblast transition contributes to the early development of diabetic renal interstitital fibrosis of streptozotocin-induced diabetic mice. Am. J. Pathol. 175, 1380-1388.

Li, J., Qu, X., Yao, J., Caruana, G., Ricardo, S.D., Yamamoto, Y., Yamamoto, H., Bertram, J.F., 2010. Blockade of endothelial-mesenchymal transition by a Smad3 inhibitor delays the early development of streptozotocin-induced diabetic nephropathy. Diabetes 59, 2612-2624.

Maleszewska, M., Moonen, J.R., Huijkman, N., van de Sluis, B., Krenning, G., Harmsen, M.C., 2013. IL-1β and TGFβ2 synergistically induce endothelial to mesenchymal transition in an NFκB-dependent manner. Immunobiology 218, 443-454.

Nawaz, M.I., Van Raemdonck, K., Mohammad, G., Kangave, D., Van Damme, J., Abu El-Asrar, A.M., Struyf, S., 2013. Autocrine CCL2, CXCL4, CXCL9 and CXCL10 signal in retinal endothelial cells and are enhanced in diabetic retinopathy. Exp. Eye Res. 109, 67-76.

Ninomiya, K., Takahashi, A., Fujioka, Y., Ishikawa, Y., Yokoyama, M., 2006. Transforming growth factor-β signaling enhances transdifferentiation of macrophages into smooth muscle-like cells. Hypertens. Res. 29, 271-276.

Österreicher, C.H., Penz-Österreicher, M., Grivennikov, S.I., Guma, M., Koltsova, E.K., Datz, C., Sasik, R., Hardiman, G., Karin, M., Brenner, D.A., 2011. Fibroblast-specific protein 1 identified an inflammatory subpopulation of macrophages in the liver. Proc. Natl. Acad. Sci. USA 108, 308-313.

Paemen, L., Martens, E., Masure, S., Opdenakker, G., 1995. Monoclonal antibodies specific for natural human neutrophil gelatinase B used for affinity purification, quantitation by two-site ELISA and inhibition of enzymatic activity. Eur. J. Biochem. 234, 759-765.

Piera-Velazquez, S., Li, Z., Jimenez, S.A., 2011. Role of endothelial-mesenchymal transition (EndoMT) in the pathogenesis of fibrotic disorders. Am. J. Pathol. 179, 1074-1080.

Sato, M., Hirayama, S., Lara-Guerra, H., Anraku, M., Waddell, T.K., Liu, M., Keshavjee, S., 2009. MMP-dependent migration of extrapulmonary myofibroblast progenitors

contributing to posttransplant airway fibrosis in the lung. Am. J. Transplant 9, 1027-1036.

Tang, R., Li, Q., Lv, L., Dai, H., Zheng, M., Ma, K., Liu, B., 2010. Angiotensin II mediates the high-glucose-induced endothelial-to-mesenchymal transition in human aortic endothelial cells. Cardiovasc. Diabetol. 9,31.

Tang, R.N., Lv, L.L., Zhang, J.D., Dai, H.Y., Li, Q., Zheng, M., Ni, J., Ma, K.L., Liu, B.C., 2013. Effects of angiotensin II receptor blocker on myocardial endothelial-to-mesenchymal transition in diabetic rats. Int. J. Cardiol. 162, 92-99.

Turner, N.A., Aley, P.K., Hall, K.T., Warburton, P., Galloway, S., Midgley, L., O'Regan, D.J., Wood, I.C., Ball, S.G., Porter K.E., 2007. Simvastatin inhibits TNFα-induced invasion of human cardiac myofibroblasts via both MMP-9-dependent and –independent mechanisms. J. Mol. Cell Cardiol. 43, 168-176.

Widyantoro, B., Emoto, N., Nakayama, K., Anggrahini, D.W., Adiarto, S., Iwasa, N., Yagi, K., Miyagawa, K., Rikitake, Y., Suzuki, T., Kisanuki, Y.Y., Yanagisawa, M., Hirata, K., 2010. Endothelial cell-derived endothelin-1 promotes cardiac fibrosis in diabetic hearts through stimulation of endothelial-to-mesenchymal transition. Circulation 121, 2407-2418.

Wynn, T.A., 2008. Cellular and molecular mechanisms of fibrosis. J. Pathol. 214,199-210.

Yang, L., DeBusk, L.M., Fukuda, K., Fingleton, B., Green-Jarvis, B., Shyr, Y., Matrisian, L.M., Carbone, D.P., Lin, P.C., 2004. Expansion of myeloid immune suppressor Gr+CD11b+cells in tumor-bearing host directly promotes tumor angiogenesis. Cancer Cell 6, 409-421.

Zeisberg, E.M., Potenta, S.E., Sugimoto, H., Zeisberg, M., Kalluri, R., 2008. Fibroblasts in kidney fibrosis emerge via endothelial-to-mesenchymal transition. J. Am. Soc. Nephrol. 19, 2282-2287.

Zeisberg, E.M., Potentia, S., Xie, L., Zeisberg, M., Kalluri, R., 2007. Discovery of endothelial to mesenchymal transition as a source for carcinoma-associated fibroblasts. Cancer Res. 67, 10123-10128.

Table 1. Monoclonal and polyclonal antibodies used in this study

Primary Antibody	Dilution	Incubation Time	Sources*
• Anti-CD31 (Clone JC70A) (mc)	Undiluted	60 minutes	Dako
• Anti-α-smooth muscle actin (Clone 1A4) (mc)	1/200	60 minutes	Dako
• Anti-CD45 (Clones 2B11 + PD7/26) (mc)	1/50	60 minutes	Dako
• Anti-S100A4 (Cat no. ab113527) (pc)	1/50	60 minutes	Abcam
• Anti-MMP-9 (Clone REGA-2D9) (mc)	1/50	60 minutes	(Paemen et al., 1995)
• Anti-CD11b (Cat no. ab75476) (pc)	1/100	60 minutes	Abcam

*Location of manufacturers: Dako, Glostrup, Denmark; Abcam, Cambridge, UK.

mc = monoclonal; pc = polyclonal

1

Table 2. Primers and probes for the study of endothelial-to-mesenchymal transition

Gene	**PrimeTime qPCR**	**Primers (5'→ 3')**	**Probe (5'→ 3')**
CD31	Hs.PT.53a.19487865	ATTGCTCTGGTCACTTCTCC	/HEX/TGTGGCGCT/ZEN/GGTCAGGTAATGG/3IABkFQ/
		CAGGCCCCATTGTTCCC	
VE-cadherin	Hs.PT.56a.4732035	TGCCCACATATTCTCCTTTGAG	/6-FAM/TGAGTCGCA/ZEN/AGAATGCCAAGTACCT/3IABkFQ/
		GAACCAGATGCACATTGATGAAG	
eNOS	Hs.PT.56a.21447620	ACGATGGTGACTTTGGCTA	/6-FAM/CAGTGGAAA/ZEN/TCAACGTGGCCGTG/3IABkFQ/
		TGGAGGATGTGGCTGTCT	
Transgelin	Hs.PT.56a.2301360.g	ATCATTCTTGGTCACTGCCA	/6-FAM/CTGCTGCCA/ZEN/TGTCTTTGCCTTCA/3IABkFQ/
		CATGTTCCAGACTGTTGACCT	
Snail	Hs.PT.56a.2984401	GCACTGGTACTTCTTGACATCT	/HEX/TTCGCTGAC/ZEN/CGCTCCAACCT/3IABkFQ/
		GGCTGCTACAAGGCCAT	
Calponin	Hs.PT.56a.38799164	CATGAAGTTGTTGCCGATGC	/HEX/CCTCGATCC/ZEN/ACTCTCTCAGCTCCT/3IABkFQ/
		TCAGCCGAGGTTAAGAACAAG	
18S	Hs.PT.45.122532.g	ATCGCTCCACCAACTAAGAAC	/6-FAM/ACCACCCAC/ZEN/GGAATCGAGAAAGAG/3IABkFQ/
		ACGGACAGGATTGACAGATTG	

*All primer/probe sets were supplied as PrimeTime qPCR assays by Integrated DNA Technologies (Haasrode, Belgium)

Legends to Figures

Figure 1. Immunodetection of endothelial and mesenchymal markers in proliferative diabetic retinopathy epiretinal membranes. A specific labeling was excluded by following the full staining procedure using an irrelevant primary antibody (A, negative control slide) (scale bar, 10 μm). Immunohistochemical staining for CD31 showing blood vessels positive for this endothelial cell marker (B) (scale bar, 10 μm). Immunohistochemical detection of fibroblast specific protein-1 (FSP-1), in stromal cells (C) (scale bar, 10 μm) and cells lining blood vessels (D and E) (scale bar, 10 μm and 8 μm, respectively). Immunohistochemical staining for α-smooth muscle actin (α-SMA) showing immunoreactivity in myofibroblasts (F) (scale bar, 10 μm) and in the vascular endothelium (G) (scale bar, 8 μm).

Figure 2. Characterization of $CD45^+$ stromal cells in proliferative diabetic retinopathy epiretinal membranes. Numerous $CD45^+$ stromal cells were detected (A) (scale bar, 10 μm). Double immunohistochemistry for CD45 (brown) and FSP-1 (red) showing co-expression in stromal cells (arrows) (B) (scale bar, 10 μm). Double immunohistochemistry for CD45 (brown) and α-SMA (red) demonstrating co-expression in stromal cells (arrows) (C and D) (scale bar, 10 μm and 8 μm, respectively).

Figure 3. Identification of $CD11b^+$ cells in proliferative diabetic retinopathy epiretinal membranes. After incubation of biopsies with antibodies against CD11b , stromal cells (A) and blood vessels (B) (scale bar, 10 μm) stained positive. Double immunohistochemistry for CD11b (brown) and α-SMA (red) (C and D, (scale bar, 10 μm and 8 μm, respectively) demonstrated cells co-expressing CD11b and α-SMA in the vascular endothelium (arrows) and in the stroma (arrow heads). Double immunohistochemistry for CD11b (brown) and matrix metalloproteinase-9 (MMP-9) (red) identified stromal cells co-expressing CD11b and MMP-9 (arrows) (E) (scale bar, 8 μm).

Figure 4. Evidence for the occurrence of endoMT in proliferative diabetic retinopathy epiretinal membranes. Immunohistochemical analysis for co-expression (arrows) of the endothelial marker CD31 (brown) and either FSP-1 (red) (A, B) (scale bar, 8 μm) or α-SMA (red) (C, D) (scale bar, 8 μm).

Figure 5. Cytokine-induced morphologic changes in retinal microvascular endothelial cells.

HRMEC were cultured in the presence of 10 ng/ml IL-1β plus 30 ng/ml TNF-α or 10 ng/ml IL-1β plus 30 ng/ml TNF-α plus 10 ng/ml TGF-β1 as described in the materials and methods section. The medium of the control cultures (Ctrl) was replaced by EBM-2 + 3%FCS without addition of cytokine(s). In alternative control cultures (VEGF), the endothelial cell type was preserved in the presence of 10 ng/ml VEGF and full endothelial cell growth medium. Representative pictures were made using a 10x phase contrast objective (scale bar 200 μm).

Figure 6. Differential endothelial and mesenchymal gene regulation in retinal microvascular endothelial cells (HRMEC) by cytokines and cytokine mixtures.

HRMEC were stimulated to undergo EndoMT as described in the materials and methods section with 10 ng/ml TGF-β1, 10 ng/ml IL-1β plus 30 ng/ml TNF-α or 10 ng/ml IL-1β plus 30 ng/ml TNF-α plus 10 ng/ml TGF-β1. Alternatively, the endothelial cell type was preserved in the continuous presence of 10 ng/ml vascular endothelial growth factor (VEGF). Changes in expression of genes related to an endothelial (endothelial nitric oxide synthase (eNOS), vascular endothelial (VE)-cadherin, CD31) or mesenchymal (calponin, snail, transgelin) cell type were detected by quantitative RT-PCR. Upregulation or down-regulation of a gene of interest was calculated relative to the control culture (Ctrl) in which the full endothelial growth medium was replaced by EBM-2 + 3%FCS without addition of cytokine(s). Results shown are mean values ± SEM from at least 4 independent experiments performed in duplicate. * or $ indicate a statistically significant upregulation or downregulation compared to the Ctrl culture, respectively ($p<0.05$ Mann Whitney U test). # indicates a statistically significant difference between two cytokine-stimulated groups ($p<0.05$ Mann Whitney U test).

Figure 7. Differential endothelial and mesenchymal marker expression in cytokine-stimulated human retinal microvascular endothelial cells (HRMEC). HRMEC were left untreated or were treated with either TNF-α (30 ng/ml), IL-1β (10 ng/ml), TGF-β1(10ng/ml), or with a combination of cytokines containing TNF-α (30 ng/ml) plus IL-1β (10 ng/ml) plus TGF-β1 (10 ng/ml) for 6 days. The levels of expression of various markers for endothelial-to-mesenchymal transition were compared by Western blot analysis. Whole cell lysates were separated by SDS-PAGE (50 µg protein/lane), blotted and markers of interest were detected by specific antibodies. Equal loading was verified by reprobing the membranes for β-actin content. Western blots are representative of three different experiments, each is performed in triplicate.

*The difference between the two means was statistically significant at 5% level of significance.

FSP-1 = Fibroblast-specific protein-1

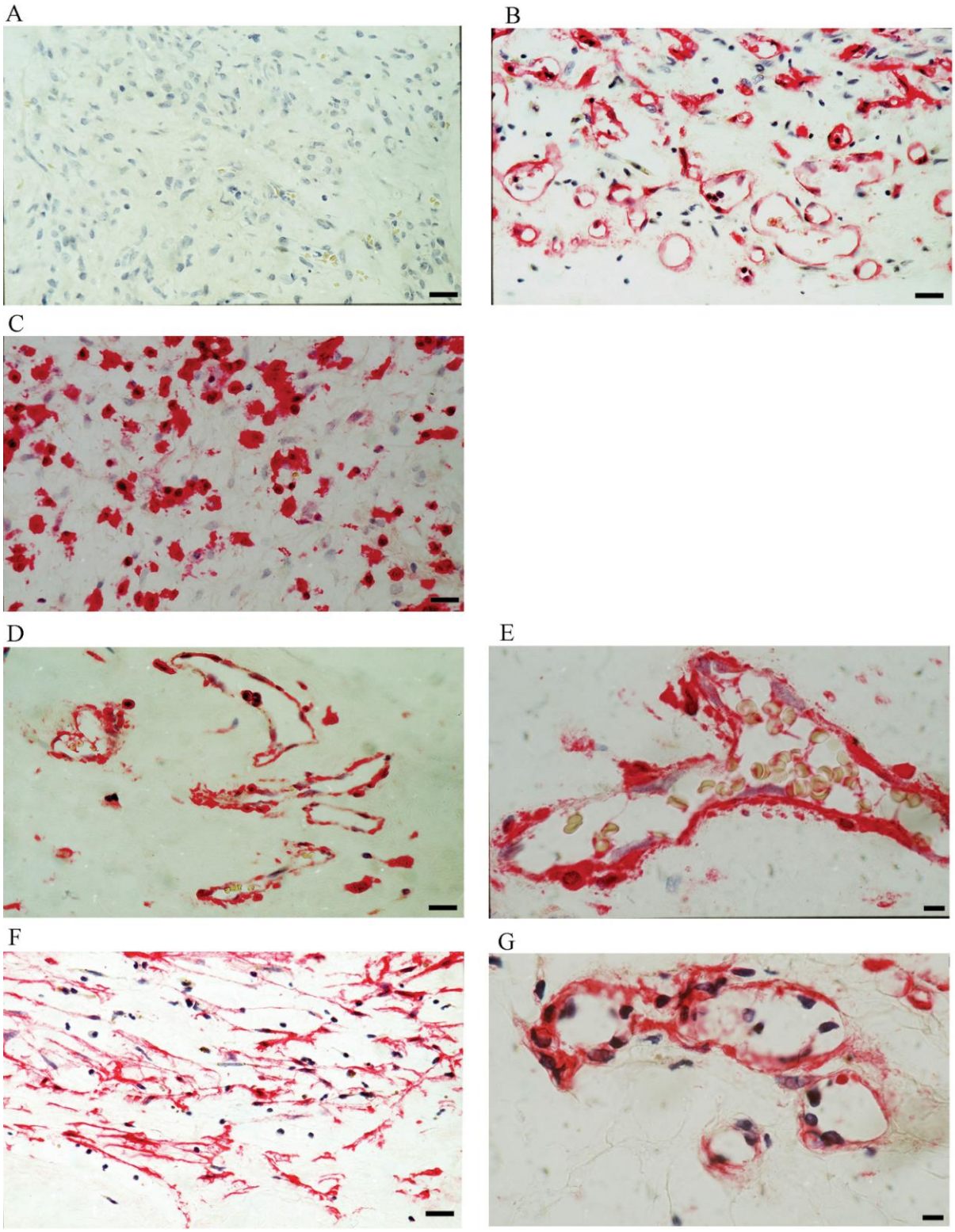

Figure 1

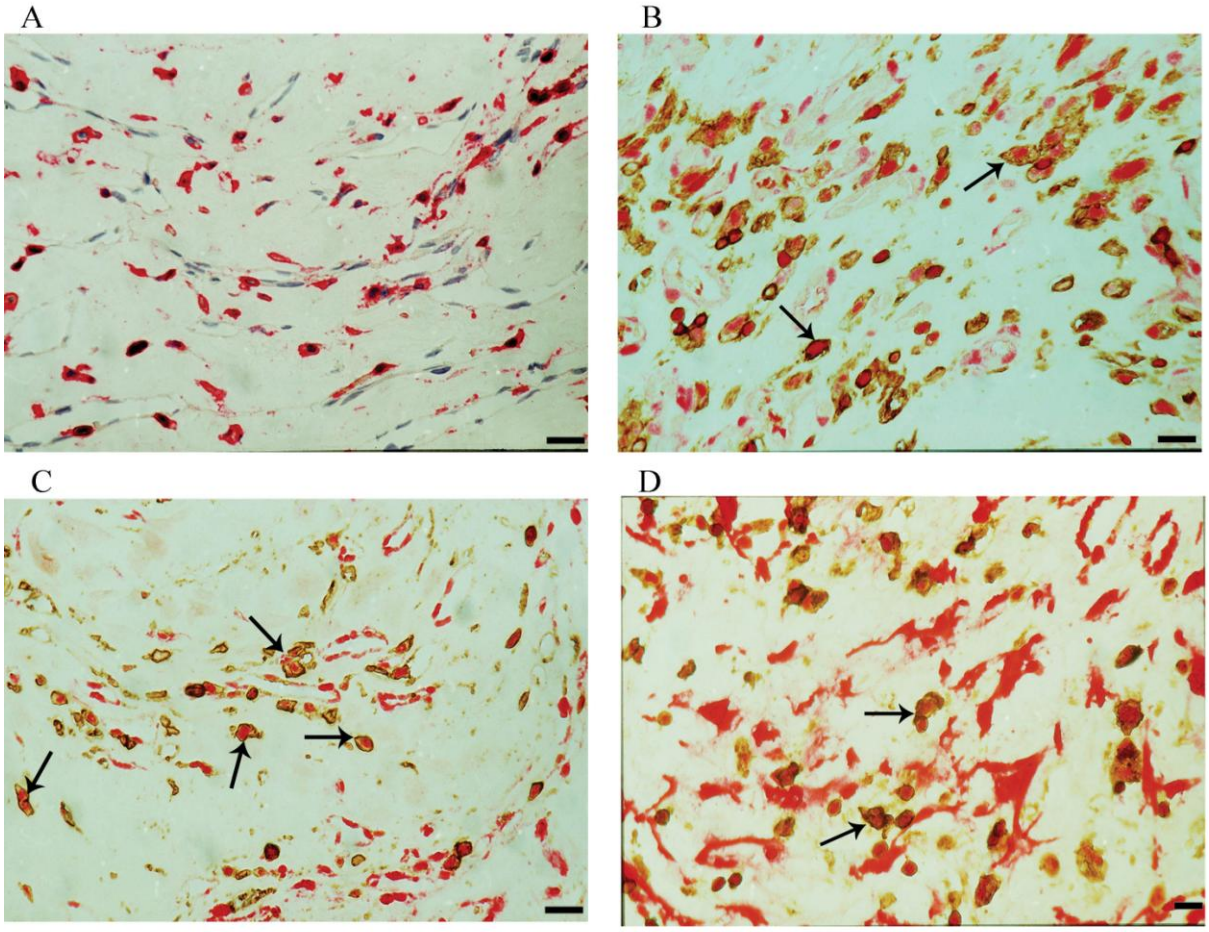

Figure 2

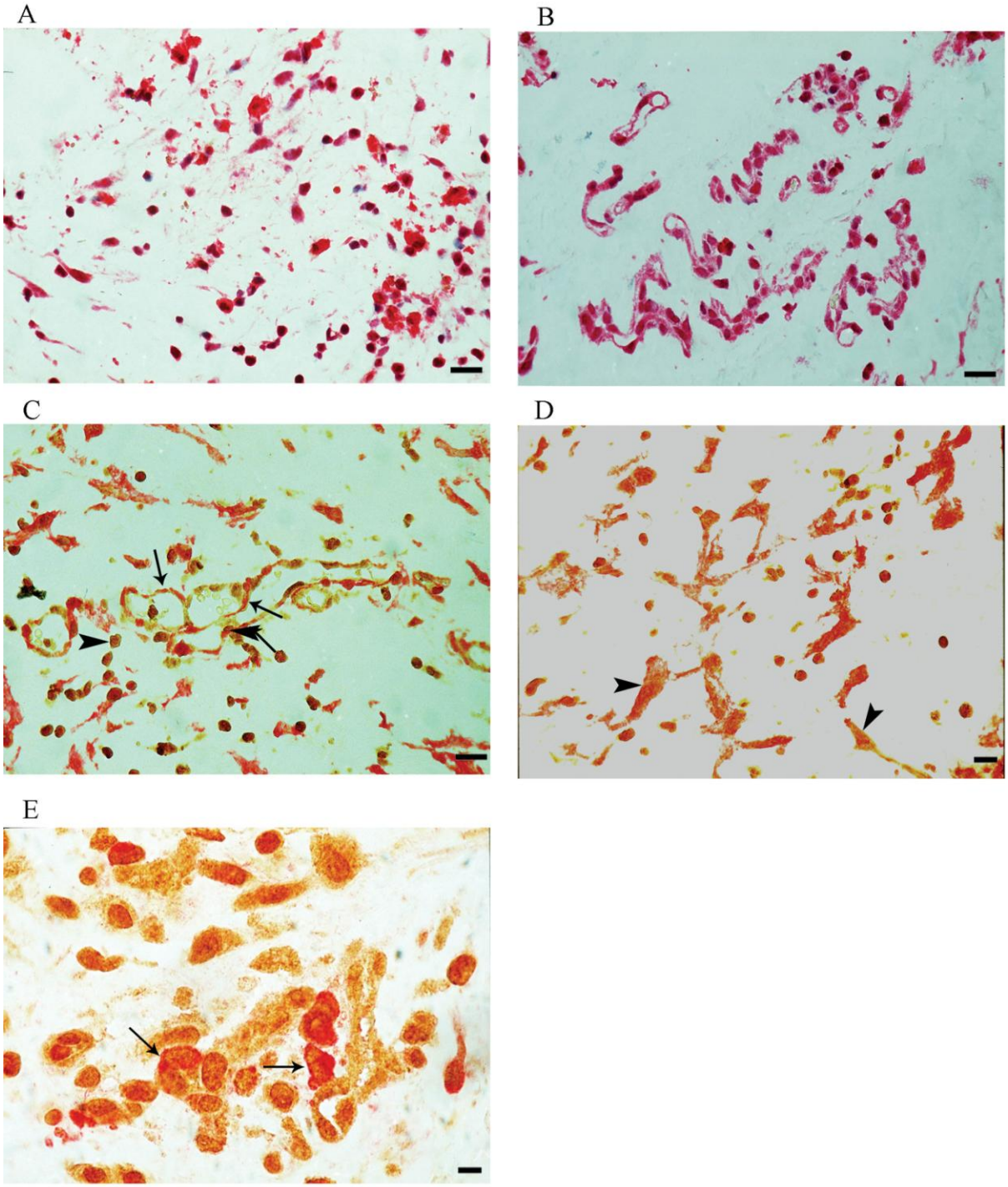

Figure 3

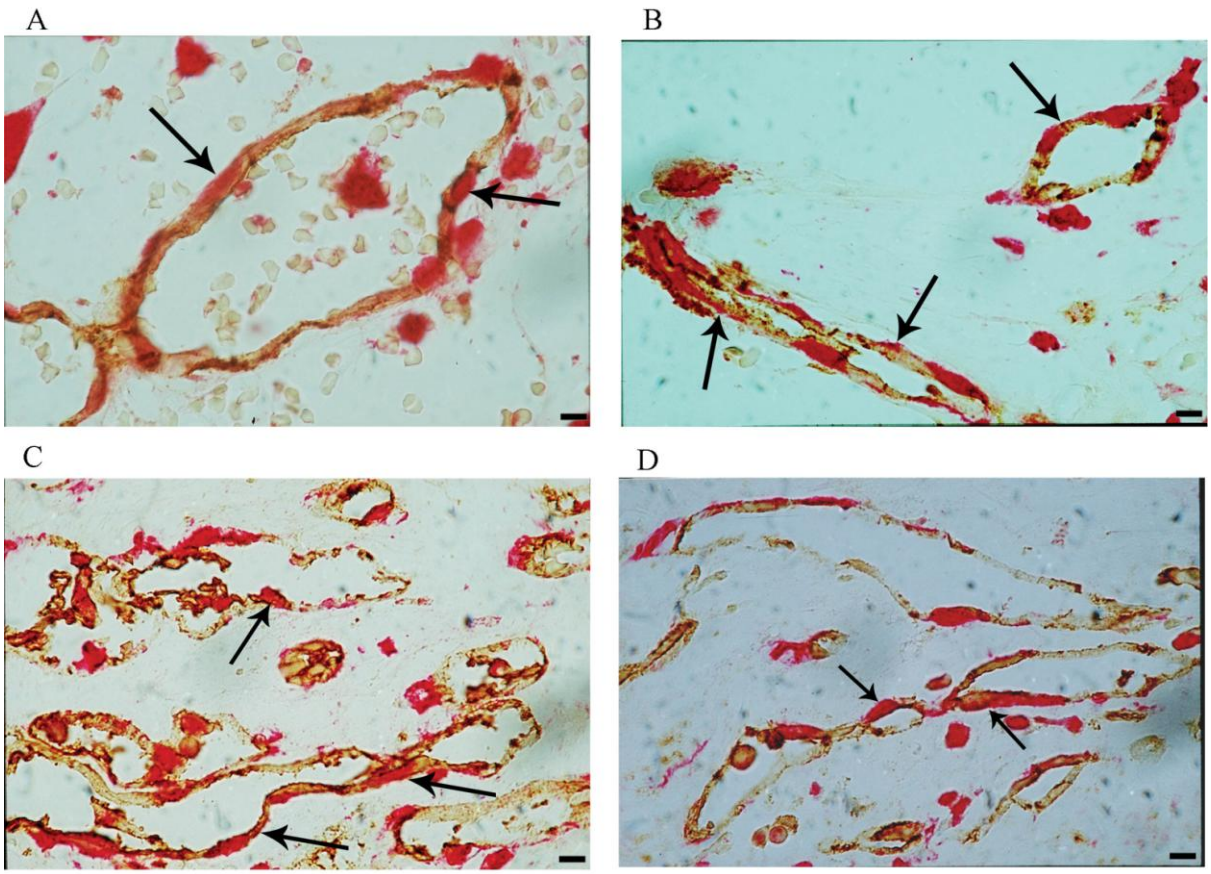

Figure 4

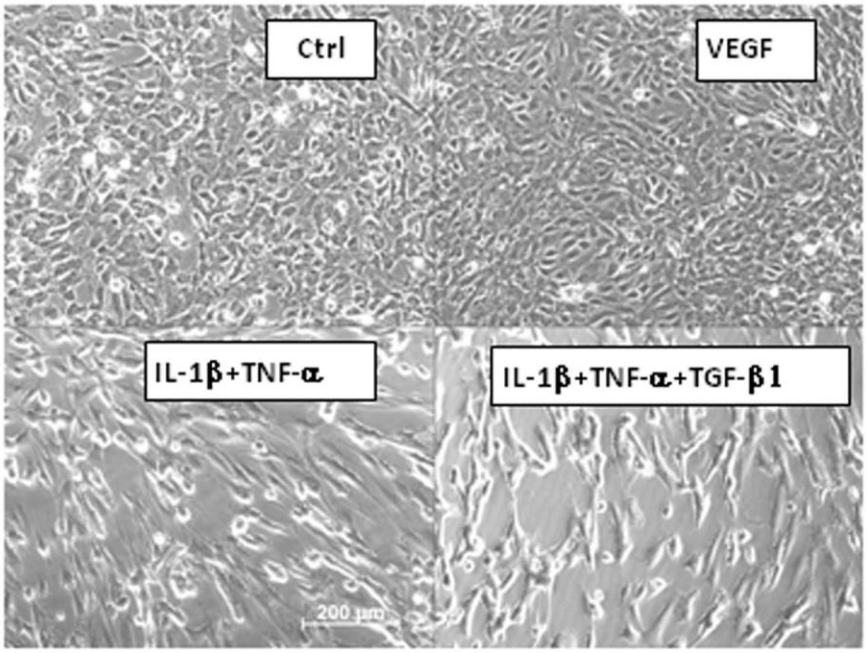

Figure 5

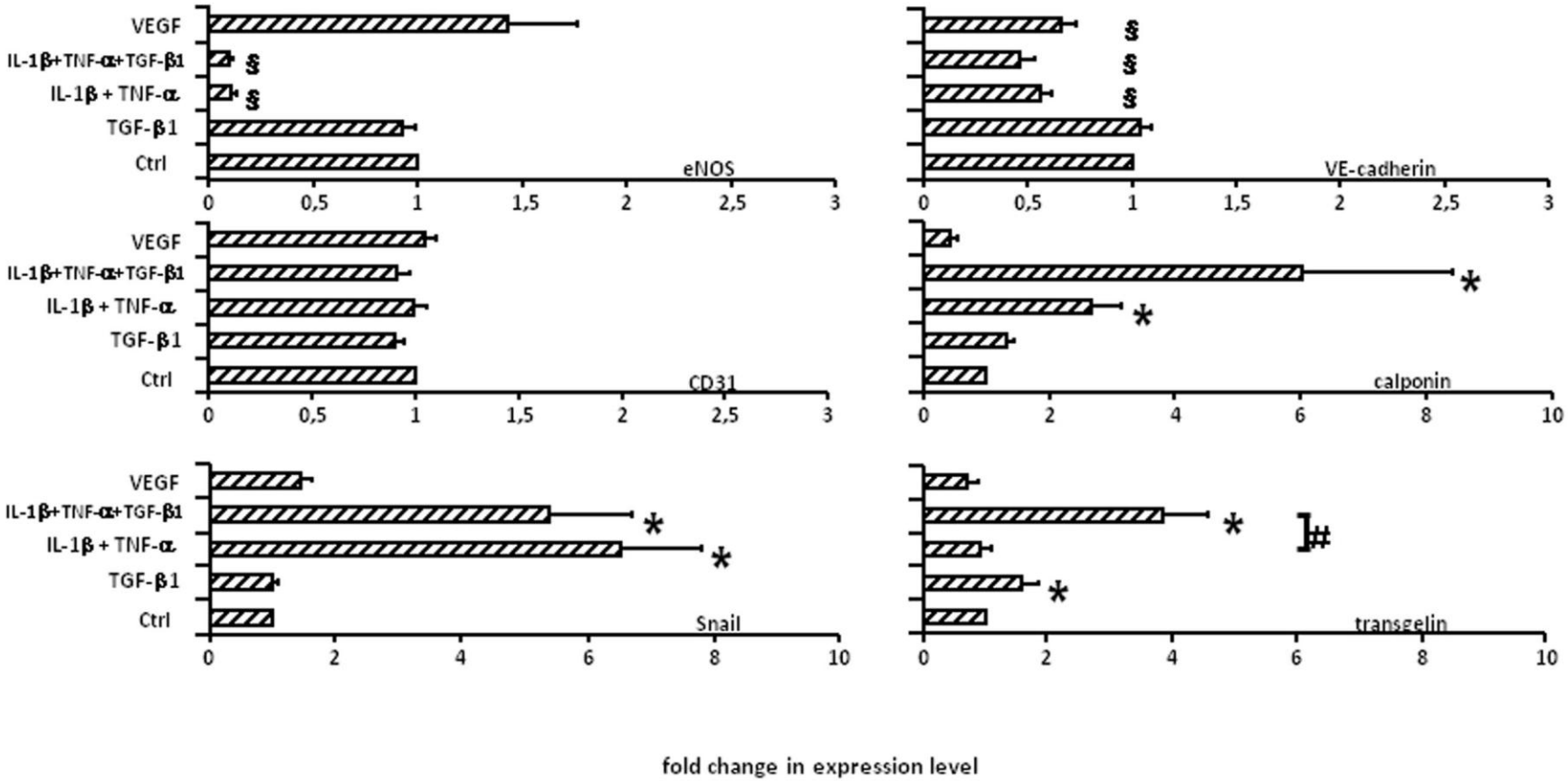
VEGF
IL-1β+TNF-α+TGF-β1
IL-1β + TNF-α
TGF-β1
Ctrl
eNOS
VE-cadherin
CD31
calponin
Snail
transgelin
$
*
#
0
0,5
1
1,5
2
2,5
3
4
6
8
10
fold change in expression level

Figure 6

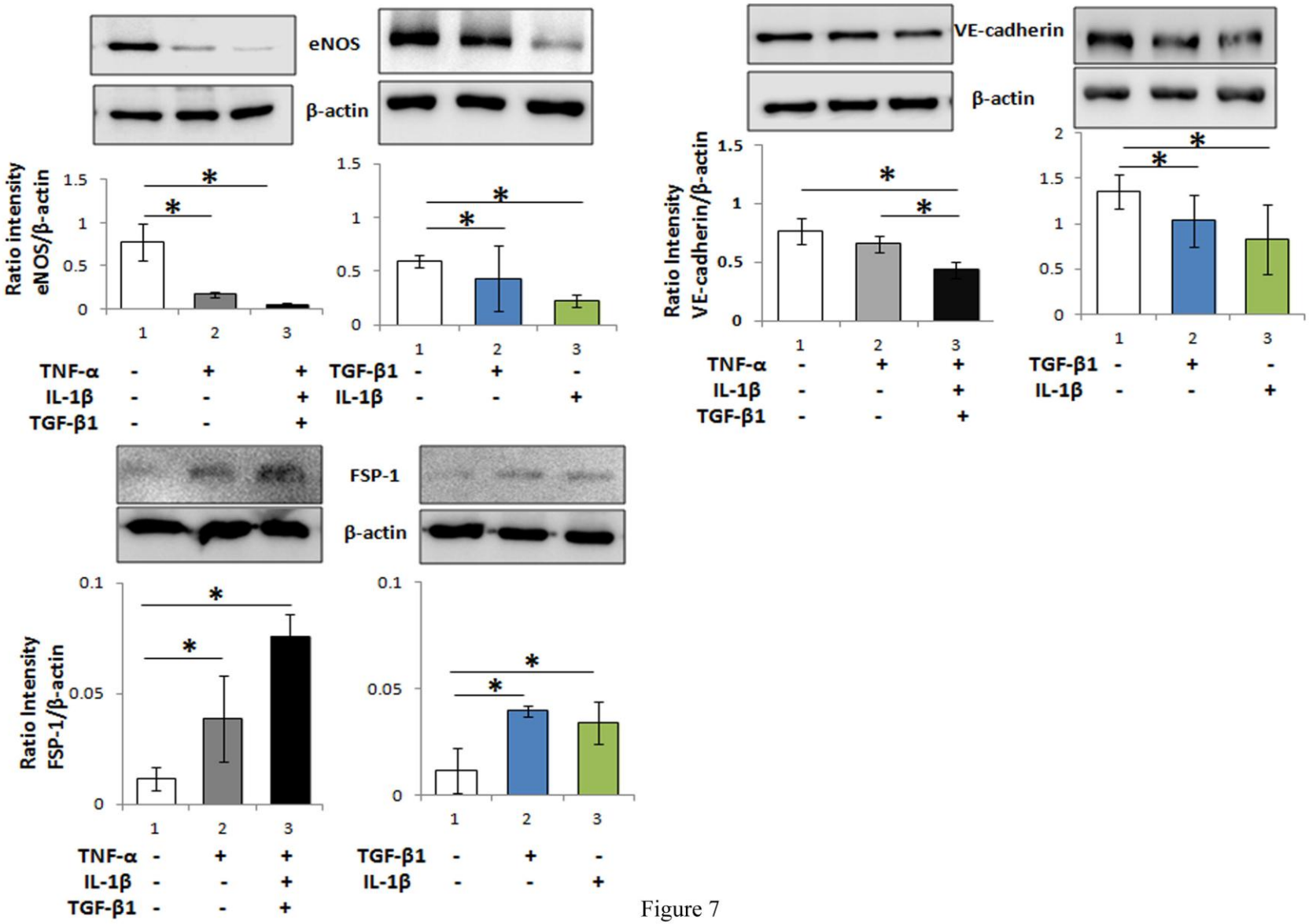
eNOS
β-actin
Ratio intensity eNOS/β-actin
TNF-α
IL-1β
TGF-β1
TGF-β1
IL-1β
VE-cadherin
β-actin
Ratio Intensity VE-cadherin/β-actin
TNF-α
IL-1β
TGF-β1
TGF-β1
IL-1β
FSP-1
β-actin
Ratio Intensity FSP-1/β-actin
TNF-α
IL-1β
TGF-β1
TGF-β1
IL-1β

Figure 7